Chapter 6
Quantification of Prediction Bounds Caused by Model Form Uncertainty

Lindsey M. Gonzales, Thomas M. Hall, Kendra L. Van Buren, Steven R. Anton, and François M. Hemez

Abstract Numerical simulations, irrespective of the discipline or application, are often plagued by arbitrary numerical and modeling choices. Arbitrary choices can originate from kinematic assumptions, for example the use of 1D beam, 2D shell, or 3D continuum elements, mesh discretization choices, boundary condition models, and the representation of contact and friction in the simulation. This works takes a step toward understanding the effect of arbitrary choices and model-form assumptions on the accuracy of numerical predictions. The application is the simulation of the first four resonant frequencies of a one-story aluminum portal frame structure under free-free boundary conditions. The main challenge of the portal frame structure resides in modeling joint connections, for which different modeling assumptions are available. To study this model-form uncertainty, and compare it to other types of uncertainty, two finite element models are developed using solid elements, and with differing representations of the beam-to-column and column-to-base plate connections: (1) contact stiffness coefficients or (2) tied nodes. Test-analysis correlation is performed by comparing the range of numerical predictions obtained from parametric studies of the joint modeling strategies to the range of experimentally obtained natural frequencies. The approach proposed is, first, to characterize the experimental variability of the joints by varying the bolt torque, method of bolt tightening, and the sequence in which the bolts are tightened. The second step is to convert what is learned from these experimental studies to models that bound the range of observed bolt behavior. We show that this approach, that combines small-scale experiments, sensitivity analysis studies, and bounding-case models, successfully produces bounds of numerical predictions that match those measured experimentally on the frame structure. (*Approved for unlimited*, *public release*, *LA-UR-13-27561*.)

Keywords Uncertainty quantification • Experimental uncertainty • Test-analysis correlation • Finite element modeling • Parametric study • Bounding calculations

L.M. Gonzales
University of Illinois at Urbana-Champaign, Urbana, IL 61801, USA
e-mail: lmgonza2@illinois.edu

T.M. Hall
Atomic Weapons Establishment, Berkshire, RG7 4PR, UK
e-mail: Tom.Hall@awe.co.uk

K.L. Van Buren (✉)
Los Alamos National Laboratory, NSEC, Los Alamos, NM 87545, USA
e-mail: klvan@lanl.gov

S.R. Anton
Tennessee Technological University, Cookeville, TN 38505, USA
e-mail: santon@tntech.edu

F.M. Hemez
Los Alamos National Laboratory, XTD-IDA, Los Alamos, NM 87545, USA
e-mail: hemez@lanl.gov

H.S. Atamturktur et al. (eds.), *Model Validation and Uncertainty Quantification, Volume 3: Proceedings of the 32nd IMAC, A Conference and Exposition on Structural Dynamics, 2014*, Conference Proceedings of the Society for Experimental Mechanics Series, DOI 10.1007/978-3-319-04552-8_6,

6.1 Introduction

Computational modeling in physics and engineering has become accepted to study the behavior of complex phenomena, especially when experiments are hindered due to time, money or safety constraints. For example, numerical models offer a cost-effective alternative to investigate parametric studies of structural damage due to the cost and safety implications associated with full-scale destructive testing [1]. Further, when pursuing new concepts for design, computational models are useful to replace the traditional design, build and test paradigm. Numerical models have become commonplace to study the behavior of a wide range of structures, such as buildings, bridges, automobiles and wind turbines, as demonstrated by their inclusion in design standards [2–4]. While useful, it is emphasized that numerical models are developed using assumptions and simplifications, thusly only being able to provide an approximation of reality. For this reason, the prediction uncertainty from numerical simulations must be quantified in order for simulation predictions to be effective in replacing or supplementing full-scale experiments.

Unavoidable sources of uncertainty exist when developing numerical models, such as experimental, parametric, numerical, and model-form (or structural) uncertainties. Reproducible and reliable experimental data are needed for use in calibration and validation assessments. However, experimental uncertainty is unavoidable, and can originate from variability of the manufactured product from design specifications, deviation of material properties from coupon properties used to represent the material behavior, and unique stress loading behaviors in critical sections of the structure [5]. Numerical uncertainty originates from the level of mesh discretization that is utilized in the model (or truncation error), round-off errors, numerical ill-conditioning, poor-quality interpolations and the lack-of-convergence of numerical solvers. In the case of truncation error, which is usually the dominant contributor, methods have been developed to produce error bounds for the resulting solution [6]. To ensure that the effect of mesh size on model output is minimal, it is typical to perform a mesh convergence study to identify the level of resolution that has an acceptably small effect on model predictions [7]. Parametric uncertainty is also commonly encountered when developing numerical models. This uncertainty represents, for example, the variability or unknown values of coefficients of a material constitutive model, energy restitution coefficients, or those of a contact condition between two surfaces. One approach is to treat these parameters as stochastic variables, for which probability laws are defined to create ranges of allowable values [8]. To identify parameters that exercise the most influence on model output, it is useful to use a phenomenon identification and ranking table, which can contribute to efficient parametric studies that include only the most influential parameters [9].

The last source of uncertainty discussed here, model-form uncertainty, is arguably more ambiguous than the experimental, numerical, and parametric uncertainties. Thus, attempts to quantify and realize the effect of model-form uncertainty have been far less encountered. Model-form uncertainty originates from assumptions or simplifications of known, or unknown, phenomena that must be represented in the numerical simulation. Assumption-making enables model building; it limits, however, the ability of the model to replicate reality [10]. When developing a model, its structural form is typically chosen based on theoretical considerations, goodness-of-fit to small-scale experiments, expert judgment, and computing constraints. This selection of a model form mitigates the lack-of-knowledge about the "best" modeling strategy that should be implemented; however, its effect on predictions often remains unknown. Some of the modeling assumptions that influence simulation results in structural dynamics include, but are not limited to: using a 1D, 2D, or 3D representation to model a component of the structure; the method through which contact and boundary conditions are represented; and the method through which external forces are applied. Due to the need for reliable simulation predictions, it is crucial to better understand the effect of model-form uncertainty on predictions.

When pursuing model-form uncertainty in structural dynamics, one area suggested as a topic of significance is the characterization of structural joints and connections [11]. After a decade-long research effort regarding the dynamics of jointed structures at Sandia National Laboratories, a recommendation is that more has to be achieved in order to quantify model-form uncertainty and "assess the cumulative uncertainty of all elements playing a role in prediction" [12]. Although much research has been conducted to understand the extent to which different joint modeling approaches accurately predict a dynamic response, more has yet to be discovered about how assumptions used in the development of these models affect numerical predictions. This work does not attempt to answer these questions for an arbitrary joint model. Instead, we propose a methodology that combines small-scale physical experimentation, sensitivity analysis and the development of bounding-case models, and apply it to a relatively simple bolted connection.

6.2 Objectives

The focus of the study is aimed at quantifying model-form uncertainty in computational models meant to simulate jointed structures. This work builds on previous studies, which have already accounted for experimental, parametric and numerical uncertainties. The novelty is to consider and quantify model-form uncertainty. This comprehensive treatment of uncertainty is useful to understand the limitations imposed by simplifications applied to numerical models, which matters greatly if numerical simulations are expected to replace full-scale experiments.

To better understand how various modeling assumptions can affect prediction accuracy, a combined experimental and numerical study is performed on the nominally symmetric portal frame structure illustrated in Fig. 6.1a. The structure is a bolted assembly of two vertical columns and a top, horizontal beam; the three-component frame is bolted to a base plate. We are interested in predicting the vibration response and, more specifically, the first four bending modes. Close-up images of the joints are shown in Fig. 6.1b, c.

Although a somewhat simple structure, predicting with accuracy the dynamic response of the portal frame can be challenging. This challenge was recognized in previous studies, in which seven groups of three students at the 2008 Los Alamos Dynamics Summer School (LADSS) independently tested and modeled the structure [13]. Seven different frames were fabricated using the same design specifications, with each group assigned an individual frame. Each group was then instructed to disassemble and reassemble the structure between experimental tests, and the students cycled through different tasks for each test: data acquisition, impact hammer, and analysis of data. Each group then developed three numerical models of the portal frame using differing model-form representations. A $\pm 3\sigma$ variability of only 4 Hz was observed in the experiments, demonstrating the overall repeatability of modal testing, and a $\pm 3\sigma$ variability of 36 Hz was observed in numerical modeling. The main contribution to the prediction bias was attributed to the modeling of the boundary condition [13]. Herein, the boundary condition of the portal frame is better controlled, in both the experimental and numerical campaigns, than what was done during the 2008 LADSS study. For simplicity, especially on the modeling side, a free-free boundary condition is imposed.

The aim of the current study is to quantify (1) the experimental variability of the measured natural frequencies due to changes in the bolt torque, and (2) the model-form uncertainty due to differing representations of the bolted connections. Experimental variability is systematically pursued by changing the bolt torque, sequence of tightening the bolts and method by which the bolts are tightened. Two finite element models are developed using solid elements to model the top beam, columns, base plate, and brackets, while the beam-to-column and column-to-base plate connections are approximated with either (1) contact stiffness coefficients or (2) tied nodes. Parametric studies of the joint modeling approximations are conducted to quantify the range of predictions obtained for each modeling strategy. The purpose of this study is not to develop a model with the "best-possible" goodness-of-fit to measurements. Instead, the goal is to identify credible prediction bounds that represent a range of situations encountered in reality.

Experimental testing explores the effect on measurements of varying control parameters of the frame structure. A non-exhaustive list of control parameters includes the suspension system of the free-free boundary condition, and the levels of bolt torque. This exploration fulfills two objectives. The first one is to characterize the overall range of measurements, that is the

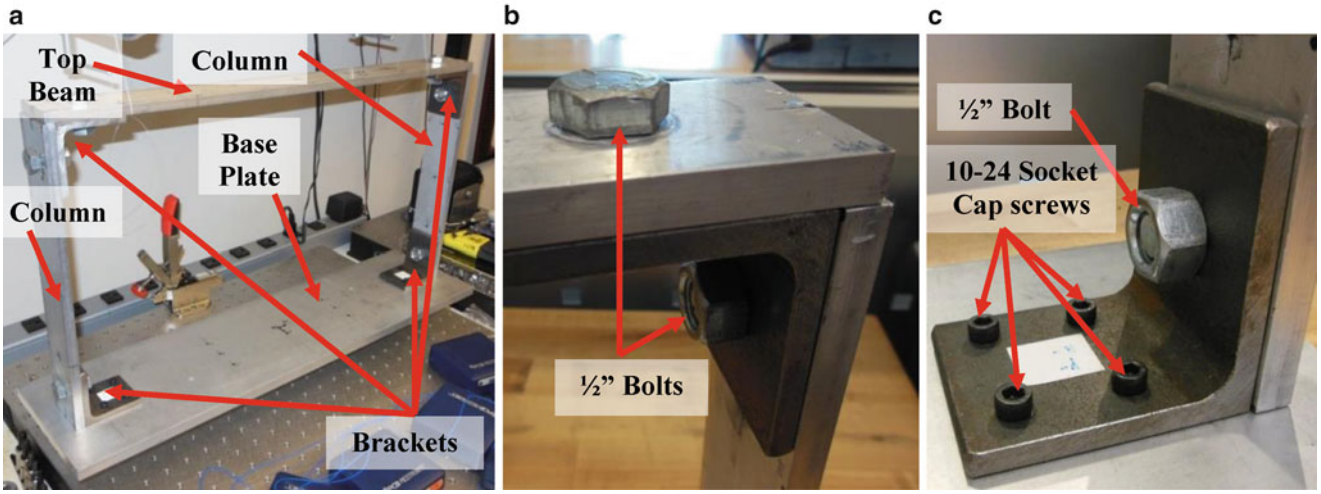

Fig. 6.1 (**a**) Portal frame (*left*), (**b**) top-side bolted joint (*middle*) and (**c**) bottom of the frame (*right*)

lower and upper bounds within which the measured frequency is expected to be observed for a similar structure. The second objective is to decompose this overall range of experimental variability to learn which control parameter, or combination of parameters, explains it. This understanding guides the development of numerical models; it is achieved through global sensitivity analysis, such as an analysis-of-variance.

6.3 Design Specifications and Experimental Setup

The portal frame structure is comprised of two aluminum columns, base plate, and top beam, and four steel L-brackets, as depicted in Fig. 6.2. The material properties of the steel and aluminum metals are given in Table 6.1. Dimensions of the portal frame are given in units of millimeters in Fig. 6.2. Note that the depth into plane is 50.8 mm, with exception of the base plate, which is 152.4 mm. The thickness of the vertical columns and horizontal top beam are identical, measuring 9.525 mm. L-brackets create the joint connections for the beam-to-column and column-to-base plate connections, with thickness of 6.35 mm. The beam-to-column connection is created using two large bolts, 12.7 mm in diameter and 25.4 mm in length. The column-to-base plate connection is created using a large bolt, also with a 12.7 mm diameter and 25.4 mm in length, to affix the column to the bracket, and four 10–24 socket cap screws, 12.7 mm in length, to connect the bracket to the base plate.

The portal frame is suspended 1 m from a support structure using fishing line; this approximates the free-free boundary condition. Based on pendulum equations as well as experimental data, the length of the suspension is deemed acceptable because the rigid body modes of the support structure are verified to be outside of the frequency range of interest. Measurement grid points for the frame are located along the centerline and edges of the vertical columns and top horizontal beam at five equally spaced locations. Grid points along the base plate are located along the centerline and at locations offset by 25 mm at four equally spaced locations between bases of the two columns.

Stiffeners are added at the top corners of the support structure to minimize the interaction of its motion with that of the portal frame. To verify that the support structure provides a sufficiently rigid boundary condition, impact modal testing is performed by impacting the portal frame and measuring the response of the support structure. Testing indicates that the fourth resonant frequency of the portal frame is around 200 Hz, whereas the first resonant frequency of the support structure is around 280 Hz. This observation confirms that the support structure is appropriate for experimental testing because interaction with the portal frame occurs outside the frequency range of interest.

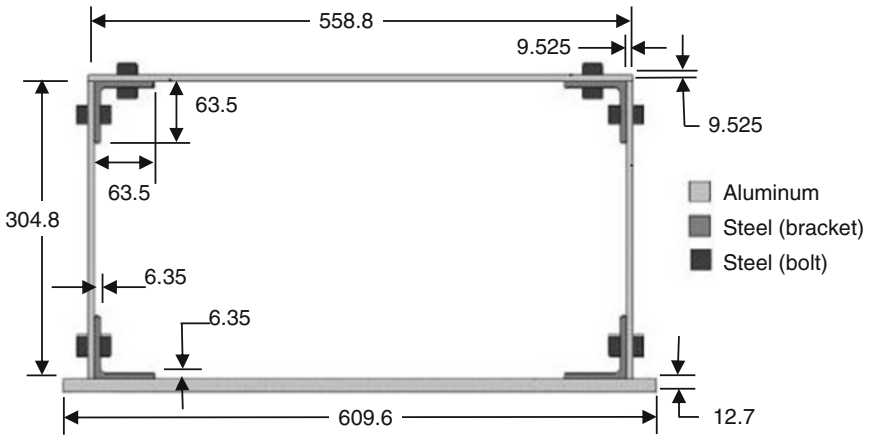

Fig. 6.2 Schematics of the portal frame structure with dimensions in millimeter

Table 6.1 Material properties of the portal frame structure

Material property	Steel	Aluminum
Young's modulus, E	200 GPa	69 GPa
Poisson's ratio, ν	0.29	0.33
Density, ρ	7861 kg/m^3	2710 kg/m^3
Shear modulus, G	80 GPa	26 GPa

6.4 Experimental Campaigns of Vibration Testing

As explained previously, the purpose of vibration testing is, first, to quantify the mode shape and resonant frequency variability and, second, to understand which physical effects control this variability. This understanding guides the development of numerical models. The response features of interest are the resonant frequencies of vibration. The mode shape deflections are also measured to ensure that the order of experimentally observed mode shapes matches the order of those obtained numerically. Relevant details of the experimental campaign are summarized here such that this paper is self-contained, as much as possible. Further details, including pre-test verification checks of experimental assumptions and preliminary vibration testing results, can be found in ref. [14].

Herein, testing is performed to explore the effect of varying the torque condition applied to the bolts. The measurements are collected with a sampling rate of 500 Hz, using a rubber impact hammer tip, and 8,192 samples. Drive-point measurements are defined by impacting only at locations of accelerometers. Throughout the experiments performed, uniaxial accelerometers are located and maintained at three measurement positions. A total of ten impacts are carried out on the structure in each of the three locations, one in each of the (X; Y; Z) directions. The bolts are numbered 1–6 starting from the bottom left bolt in Fig. 6.2 and moving clockwise around the structure. It is verified that these experimental settings provide sufficient data quality; they are kept identical for all experimental campaigns to remain consistent as much as possible between the different measurements.

6.4.1 Effect on the Measured Response of Varying the Bolt Torque Level

The first experimental study conducted is to determine how the bolt torque level affects the structural behavior of the portal frame. Torque is increased from 4.52 to 9.04 Nm and 18.08 Nm. Impact hammer testing is repeated for each level of torque. The sequence in which the bolts are tightened remains the same for all tests performed, so as to not introduce additional variability to the experimental results. The tightening order used is 2-3-6-4-5-1.

Table 6.2 reports the average values of resonant frequencies obtained at each torque level. The trend observed is unambiguous: as the torque is increased, the portal frame becomes stiffer and the resonant frequencies begin to rise. Figure 6.3 displays a visual comparison of this trend by reporting the behavior of normalized frequency changes. The normalized changes are defined as deviations from the average frequency for each mode. The measurements of Table 6.2 are used to calculate the normalized frequencies for each mode. Normalized values better capture an overall trend, like those shown in Fig. 6.3. Table 6.2 and Fig. 6.3 indicate that the resonant frequencies of modes 1, 2 and 4 are affected by changes to the bolt torque level, while those of mode 3 remain nearly unchanged. A reason why modes 1, 2 and 4 are more sensitive to the bolt preload might be that their deflections involve significant shearing or frictional effects at the joints. As torque increases, so does the normal force being applied to the bracket and beam surfaces in contact with each other, and so does friction. Therefore, it makes sense that deformation modes involving shearing and friction would be more sensitive to changes in bolt torque, at least, in the low frequency range. The third mode, on the other hand, involves out-of-phase bending that might pull apart beams in contact in the direction normal to their surfaces. If so, then the third mode would be less sensitive to bolt torque while it is influenced, instead, by bolt material properties.

6.4.2 Effect on the Measured Response of Changing How the Bolt Is Torqued

Having developed an understanding of how bolt torque affects the modal frequency data, the method by which the bolts are tightened is considered next. The initial bolt torque study considered the behavior of the portal frame when the bolts are tightened directly to the specified values of torque used in the experiments. Here, additional testing is conducted to observe the extent to which gradually increasing the bolt torque provides a different level of experimental variability as opposed to directly increasing the bolt torque.

Table 6.2 Resonant frequencies obtained by changing the bolt torque level

	Measured resonant frequency (Hz)			
Torque level (Nm)	First—shearing	Second—torsion	Third—out-bending	Fourth—in-bending
4.52	58.9	97.6	104	172
9.04	62.8	101	104	178
18.08	67.9	102	105	186

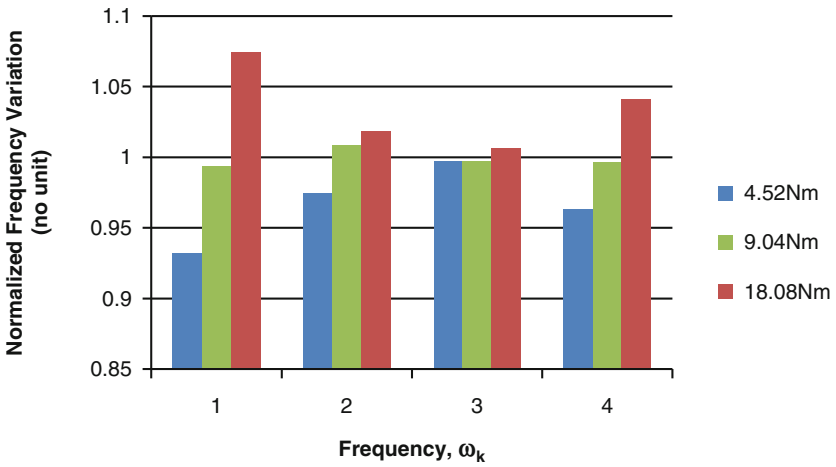

Fig. 6.3 Normalized frequencies obtained by changing the bolt torque level

Table 6.3 Definition of tightening sequences

Experiments 1–2		Experiments 3–4		Experiment 5	
Sequence	Bolt order	Sequence	Bolt order	Sequence	Bolt order
1	2-3-6-4-5-1	3	6-2-3-1-4-5	5	1-6-2-5-3-4
2	2-3-4-5-6-1	4	1-2-3-4-5-6		

The torque levels are increased incrementally by steps of 1.13 Nm at each bolt location. The same sequence of bolt tightening as the one used in the previous study is used; it avoids biasing the comparison by introducing another factor in the analysis. The incremental tightening is performed to ensure that each bolt has a snug fit when tightened. Analysis of the results determines that the bolt tightening method has negligible, if any, effect on the frame's resonant frequencies.

6.4.3 *Effect on the Measured Response of Changing the Bolt Tightening Sequence*

The experiments discussed in the previous two sections used a constant sequence in which the bolts are tightened. Here, the effect that the tightening sequence has on experimental variability is investigated. The study considers five different sequences at each one of the three torque levels. Table 6.3 shows the five sequences considered, where the bolt numbers are defined earlier. For each experiment performed in this study, the bolts are tightened from finger-tight directly to the torque level specified.

The bar graph in Fig. 6.4 shows the normalized frequencies obtained for the five tightening sequences at the 4.52 Nm torque level. There is no visible trend that would suggest that the bolt tightening sequence affects resonances of the portal frame in a systematic and consistent way. Furthermore, the changes observed remain small compared to those illustrated in Fig. 6.3, where the effect of bolt torque level is investigated. However it is observed that the bolt tightening sequence provides greater experimental variablity than the procedure used to tighten the bolts.

6.4.4 *Overall Assessment of Experimental Variability*

An Analysis-of-Variance (ANOVA) is conducted next to confirm the observations made in Sects. 6.4.1, 6.4.2 and 6.4.3. The ANOVA is a statistical method that expresses the total variance of the measured frequencies of the portal frame, as a decomposition of partial variances [14].

Results of the main-effect ANOVA are given in Fig. 6.5. Statistics for the tightening procedure are omitted because the R^2 values are small compared to the others. For convenience, the R^2 values are normalized mode-by-mode to add to 100 %. As postulated, the level of torque has the greatest influence on resonant frequencies of modes 2, 3 and 4. Contributions to the variability of the first resonant frequency (shearing mode, shown in the left-most bar) are shared almost equally between the bolt torque level and tightening sequence. This suggests that reaching a high level of test-analysis correlation might be more difficult for the shearing mode because the physical measurements are influenced by a factor that is more involved to simulate numerically. It is emphasized that these results are from a main-effect analysis. As such, they do not capture the influence on frequency variability of a potential interaction between two, or more, factors.

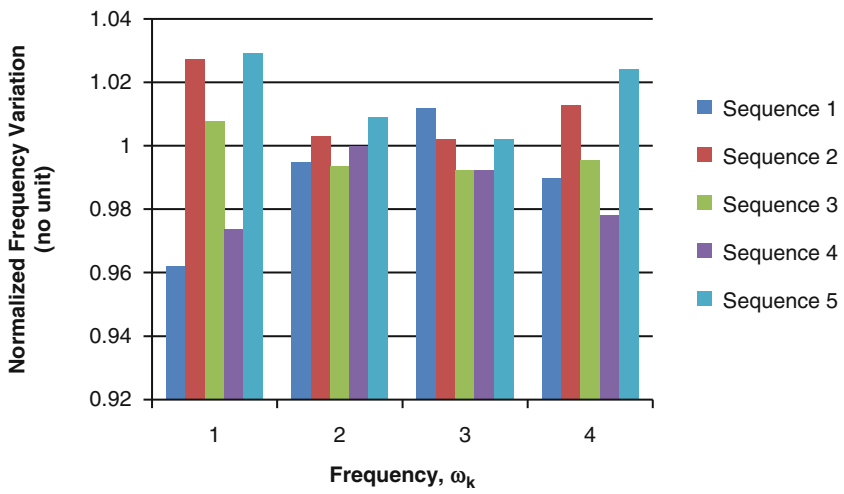

Fig. 6.4 Normalized frequencies obtained by changing the bolt tightening sequence at the 4.52 Nm torque level

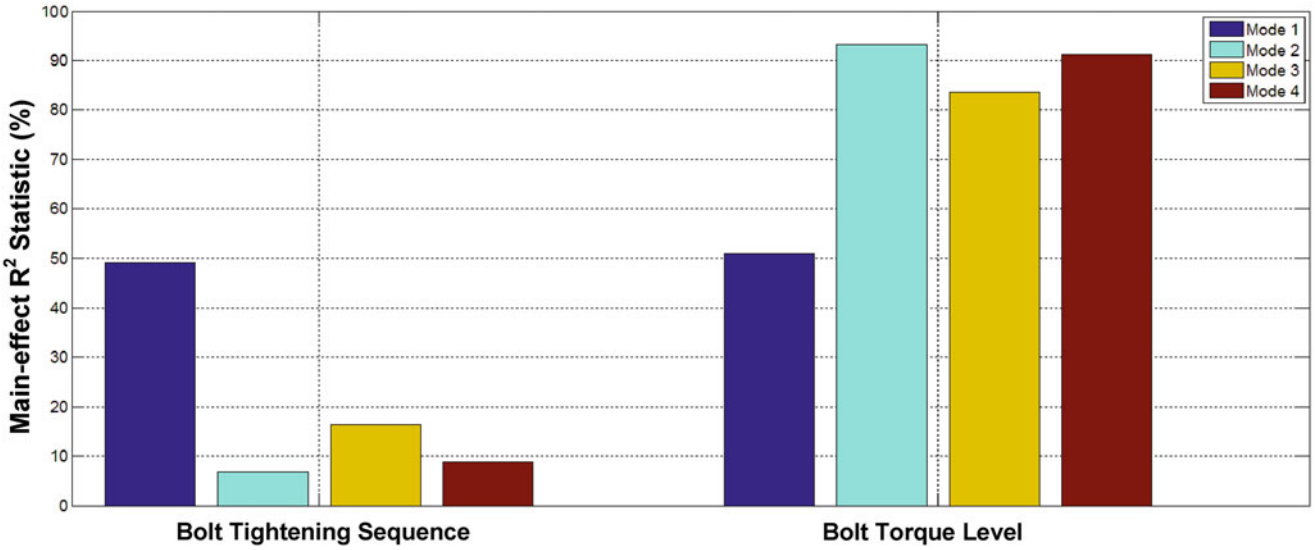

Fig. 6.5 Main-effect decomposition of measured resonant frequency variability

Table 6.4 Overall ranges of resonant frequency variability (from measurements)

	Measured resonant frequency (Hz)							
	Shearing		Torsion		Out-bending		In-bending	
Torque level (Nm)	Low	High	Low	High	Low	High	Low	High
4.52	58.8	63.0	97.5	99.0	102	104	170	178
9.04	62.8	66.6	99.8	101	104	105	180	178
18.08	66.3	71.6	102.0	103	105	106	183	193

Results from the statistical analysis reaffirm the empirical observations of the previous three sections. Increasing the bolt torque increases the overall stiffness of the structure, which causes the resonant frequencies to increase as well. The sequence in which the bolts are tightened has minimal influence on resonant frequencies, except for the shearing mode.

To conclude the analysis of experimental campaigns, the overall ranges of measured resonant frequencies are reported in Table 6.4. These lower and upper bounds are used in the following to assess the prediction accuracy of finite element model predictions. The third, out-of-phase first bending, mode is least sensitive to the experimental conditions tested. The difference in variability observed for the first four resonant modes might be explained by the shearing "action" in the joints of mode shapes, where resonant frequencies with more variability correspond to deformation shapes with more shearing at the contact surfaces. Findings, such as this one, are useful to guide the development of numerical models.

6.5 Finite Element Models of the Portal Frame

After assessing the experimental variability, and studying which factors are most influential to change the resonant frequency values, we proceed with the development and "validation" of numerical models. Model validation, here, has a particular meaning. The goal is not to demonstrate, through a combination of parameter study and calibration, that model predictions can reproduce the measurements. Instead, the objective is to develop numerical models whose predictions "envelope" the experimental variability assessed in Sect. 6.4.

To do so, two Finite Element (FE) models are developed using the modeling and analysis software Abaqus™ to study model-form uncertainty associated with the behavior of beam-to-column and column-to-base plate connections of the portal frame structure. All structural components (horizontal beam, vertical columns, base plate, attachment brackets) are modeled using three-dimensional, 8-noded solid elements.

6.5.1 Development of the "Bounding-Case" Finite Element Models

Instead of developing a single FE model whose predictions reproduce the measurements as best as possible, our goal is to assess the effect that competing model-form assumptions have on predictions. This goal is achieved by developing two FE models. The starting point is the three-dimensional geometry represented with solid elements mentioned above. Assumptions are then formulated to describe the behavior of beam-to-column and column-to-base plate connections.

From the experimental campaigns discussed previously, it is clear that the bracket connections allow for some degree of compliance at contact surfaces. This is evident from the influence exercised by procedures such as the tightening sequence. In the presence of an "infinitely rigid" interface that exhibits no compliance, there would be no mechanism for the tightening sequence to exercise any influence at all. On the other hand, we have observed that resonant frequency values are strongly influenced by the level of applied torque. It means that, even though the jointed connections might introduce some compliance, the contact condition is also sensitive to the normal preload applied by the bolts.

From these observations, the collection of models, which could be developed to represent the bracket behavior, can be defined along two dimensions. The first dimension is the degree of compliance of the joint and the second dimension is the region over which this compliance exercises an influence. In this study, a contact stiffness strategy is used to explore the compliance of the joint and a tied node representation is utilized to explore the region of action of the joint.

The contact stiffness representation of the frame uses three-dimensional translational spring elements at coincident nodes of the bracket-to-beam, column, or base plate connection. Spring coefficients are specified in the normal (k_{nn}) and two orthogonal shear (k_{ss} and k_{tt}) directions; these are used to parameterize the FE model as they are non-physical parameters and are, therefore, unknown. The entire contact surface is jointed in this manner. In the second case, nodes of the two surfaces in contact are tied together, which is a condition that does not allow for any relative displacement. The tied nodes are only active over a circular region of given radius, with the radius allowing parameterization of the FE model.

Other modeling strategies, for example, using solid elements to represent the bolts explicitly or imposing "fictitious" springs over a radius-of-influence, offer further modeling alternatives. Only the above two strategies are investigated because, first, they define bounding cases of how the jointed connections might behave and, second, they represent simplifications commonly encountered in the modeling and simulation community.

6.5.2 Quantification of Numerical Uncertainty for the Finite Element Simulations

A mesh refinement study is carried out on various subassemblies of the model in order to determine an approximate value for the truncation error of model predictions. This is carried out by creating models with varying sized meshes and performing calculations to determine the errors on each mesh size. The mesh sizes chosen all have an aspect ratio for all elements of near one, with the size difference corresponding to the number of elements through the smallest thickness in the subassembly. Models are created with 1, 2, 3, 4 and 8 elements through thickness. A first mesh refinement study is applied to a straight beam with rectangular cross-section, 152.4 mm long, 25.4 mm wide, and 9.5 mm thick. A second refinement study is performed using the bracket connection of the portal frame. Discretizing the structural components with three finite elements through the thickness provides a truncation error of 5.64 % for the beam problem and 2.34 % for the bracket connection problem. At three elements through thickness, 5.64 % error is the largest found across all studies. Using two elements through the thickness leads to the error of 13.27 % for the straight beam problem, which is deemed too large. Computing, on the other

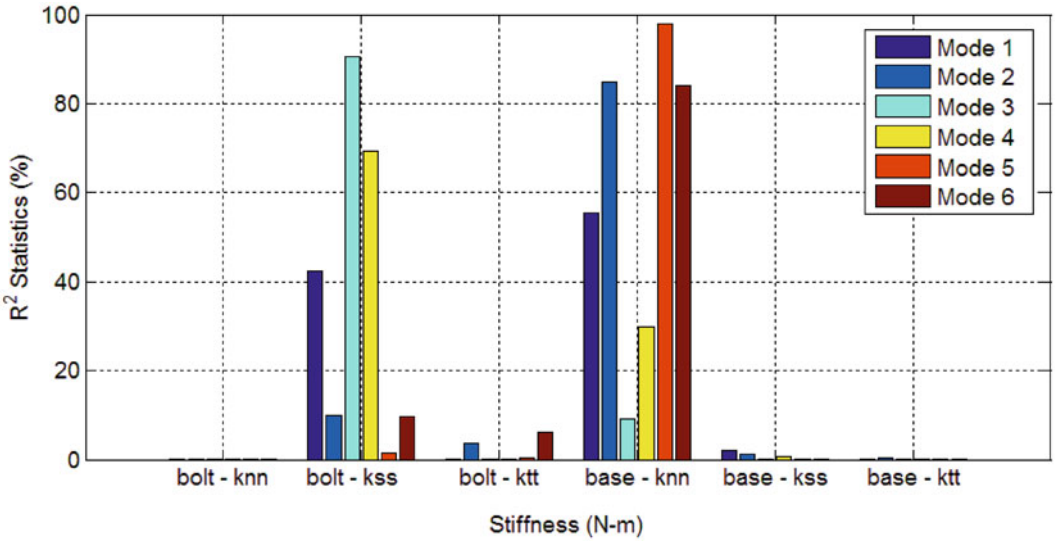

Fig. 6.6 Main-effect ANOVA of predicted frequencies (contact stiffness FE model)

hand, with four through-thickness elements greatly increases the time-to-solution. With these considerations, a discretization with three elements through the thickness is selected for the portal frame [14].

The resulting, nominal FE model features a total of 105,400 nodes and 75,534 finite elements. A modal analysis performed to extract the low-frequency mode shapes is solved in ≈1 min on a typical PC workstation, which is fast enough to perform a few hundred runs for the parameter studies presented next. This discretization, with three through-thickness elements (top beam, side columns, brackets, base plate), is identical for all runs performed.

6.5.3 Parameter Study of the Contact Stiffness Representation

Spring coefficients of the contact stiffness representation are investigated next. The first step is to decide ranges over which these values must be varied. It is observed that, for values lower than 10^{+10} N/m, the order of the modes changes. This is an indication that the contact surface condition deviates from the experimental condition and, therefore, the spring coefficients used in the FE model are not appropriate. On the other hand, the resonant frequencies asymptote to constant values when the spring coefficients exceed 10^{+15} N/m. It indicates that the jointed connection is essentially "rigid" and further increasing the spring stiffness values has no effect. These two observations set the lower and upper bounds of stiffness coefficients to the range (10^{+10} N/m; 10^{+15} N/m). The parameter study is pursued using this range of values.

To keep the study to a manageable size, all of the bolts of the bracket-to-vertical column and bracket-to-top beam connections are grouped together and assigned the same stiffness values in the normal, shear and tangential directions. These coefficients are denoted by k_{nn} (normal), k_{ss} (shear) and k_{tt} (tangential). Similarly, the 10–24 socket cap screws of the bracket-to-base plate connections are grouped together and assigned the same stiffness values k_{nn}, k_{ss} and k_{tt}. This parameterization of the model gives six spring coefficients where each is varied within the range (10^{+10} N/m; 10^{+15} N/m).

A two-level, full-factorial design-of-computer-experiments is defined to propagate the ranges of spring stiffness values through the model. Predictions are used to observe the effect on the first six resonant frequencies of changing one spring at a time. This analysis is similar to the main-effect analysis applied to measured resonant frequencies in Sect. 6.4.4.

The ANOVA results of Fig. 6.6 clearly indicate that one of the bolt shear parameters ("bolt k_{ss}") and the base plate normal stiffness ("base k_{nn}") are the two most influential parameters for the six resonant frequencies. They must be considered to quantify the prediction uncertainty. Observing that the bolt shear stiffness coefficient is one of the most influential parameters of the FE model matches the intuition gained from experimental campaigns, where it is observed that most of the target modes are sensitive to shearing effects of the jointed connections. The ANOVA also indicates that the other four stiffness coefficients can be eliminated from further consideration since varying them from the lower to upper bounds does not significantly change the frequency predictions. These four parameters are kept constant and equal to mid-range values ($3.16 \times 10^{+12}$ N/m, mid-point on a $\log_{10}$-scale).

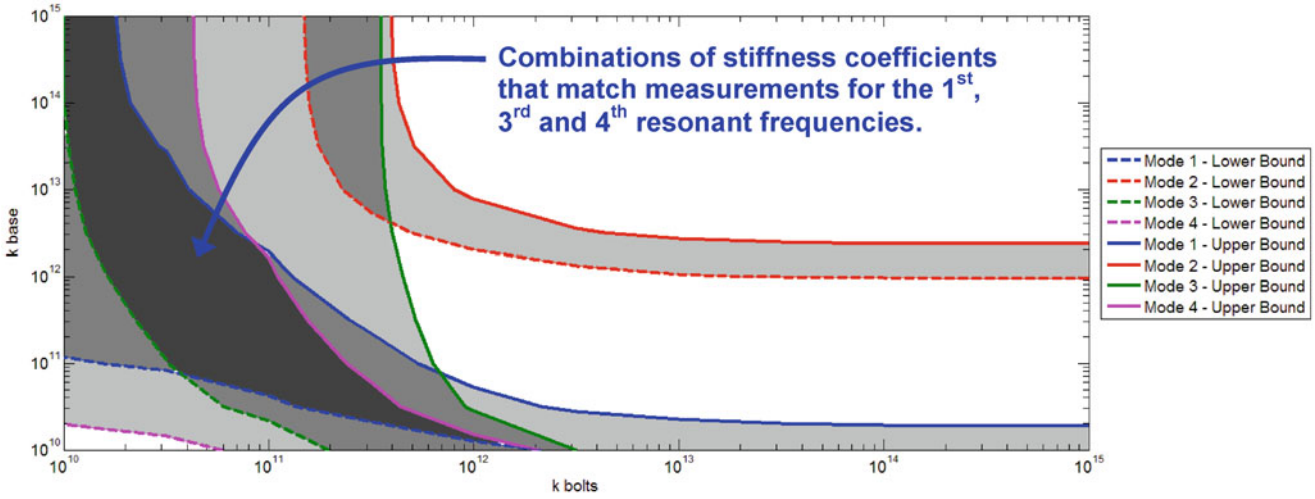

Fig. 6.7 Filled contours indicating where predictions are within measurement bounds for the 4.52 Nm torque case

Having eliminated four of the six spring coefficients, an 11-level, full-factorial design is analyzed next, where all of the bolt coefficients are grouped together and, likewise, all of the base plate coefficients are grouped together. The two groups are denoted by k_{Bolt} and k_{Base} that correspond, respectively, to the symbols "bolt k_{ss}" and "base k_{nn}" used previously. Because it features more than two levels per parameter, this second design can capture potential nonlinear effects of varying one of the stiffness coefficients, or two coefficients simultaneously. The design results in an additional $11^2 = 121$ runs of the FE model.

The results of this study are used to observe the combinations of spring coefficients (k_{Bolt}; k_{Base}) that provide frequency predictions that "match" the measurements. "Matching," here, is not an attempt to reproduce the measured values as best as possible; our criterion is, instead, to produce predictions that reside within the lower and upper bounds estimated from the experimental campaigns. This is achieved by determining the pairs of coefficients that give a particular frequency, then plotting the iso-frequency values that correspond to the lower and upper bounds of measurements (see Table 6.4). Two contours are obtained from this process, corresponding to the lower and upper bounds of experimental observations. Figure 6.7 illustrates results of the process, repeated for the first four modes.

Regions of Fig. 6.7 shaded in light grey indicate combinations of spring coefficients (k_{Bolt}; k_{Base}) that comply with the criterion "predict a frequency within the experimental bounds" for a given frequency and torque level. Darker shades of grey highlight regions where multiple selection criteria overlap.

It can be observed that a common overlap can be found for the first, third and fourth resonant frequencies. This is true for all torque levels. No pair of stiffness coefficients (k_{Bolt}; k_{Base}) is found, however, that provides a common overlap for the second mode (torsional mode). The inability to match all four frequencies simultaneously suggests that the FE model parameterization is not appropriate to capture torsional effects. Varying the stiffness coefficients independently, instead of grouping them together, has not been attempted due to the time constraint of a study limited to 10 weeks. In addition, ANOVA results from the experimental testing suggest that the level of bolt torque is most influential. The fact that the method and sequence of bolt tightening are of lesser influence experimentally suggests that all of the bolts maintain a similar fit, which makes it reasonable to group all bolts together. Not being able to capture the second mode well might also suggest a fundamental flaw with the contact stiffness representation.

6.5.4 Parameter Study of the Tied Node Representation

The parameter study of the tied node representation is similar to the previous one, except that it involves a single parameter: the radius-of-influence of the bolted joint. Here, the radius is incrementally increased from 5 to 30 mm. The lower bound of 5 mm is selected because it defines an area smaller than the surface area of the bolt head/nut. The surfaces defined for $5 \text{ mm} \leq r \leq 25$ mm provide a circular contact. The upper bound of 30 mm defines a circle that falls partially outside the face of the bracket, whose dimension is 63.5 mm by 50.8 mm. The tied condition is applied only to nodes of the bracket face that overlap with those of the surface-of-influence. Since there is only one parameter to consider, the study is simpler than previously. The goal is nevertheless similar: search for radius-of-influence values that define FE models whose predictions reside within the lower and upper frequency bounds assessed experimentally.

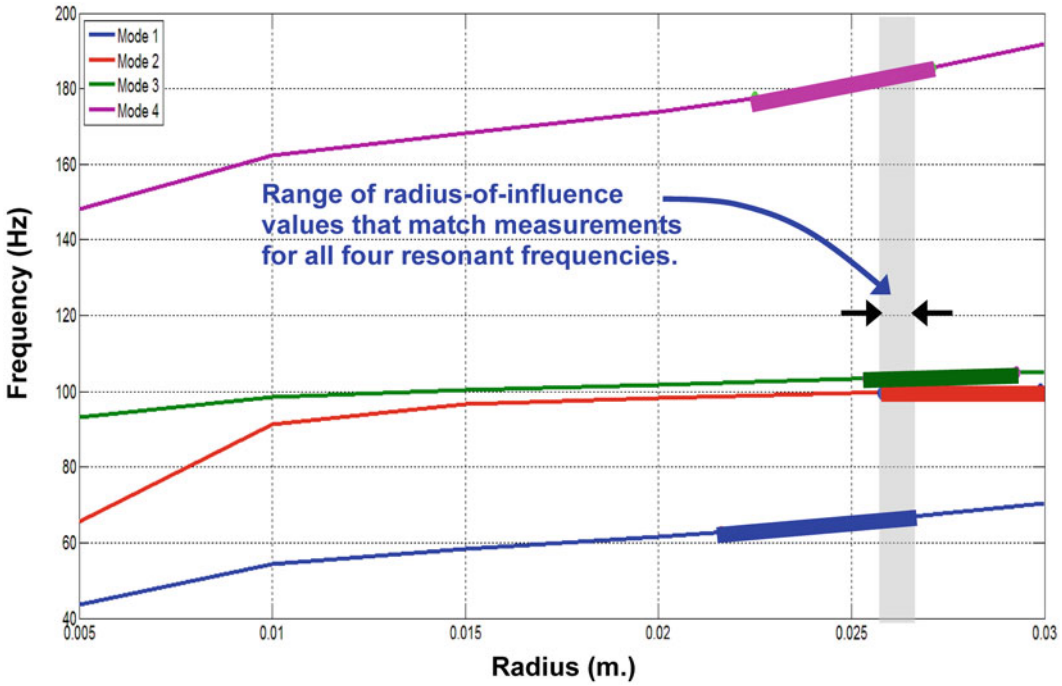

Fig. 6.8 Parameter study of the radius-of-influence for the 9.04 Nm torque case

Figure 6.8 displays how the first four resonant frequencies change when the radius-of-influence varies within the interval (5 mm; 30 mm). All radii of bolt connections are varied in a similar manner. Due to computational resource and time constraints, the scenario where each bolted connection would define its own radius-of-influence is not analyzed. For comparison, measured frequency ranges obtained with the 9.04-Nm torque are indicated with thicker solid lines. Only the 9.04-Nm torque case is illustrated in Fig. 6.8 because the other cases give similar observations.

As expected, the resonant frequencies increase as the radius-of-influence increases, causing the joints to behave more rigidly. Frequencies of the first, second and fourth modes experience significant changes in value with the increase in contact radius. Frequencies of the third mode (out-of-phase bending mode) do not experience as much change. This trend is consistent with the results of physical testing where it is observed that the third-mode resonant frequency exhibits the smallest variance at all bolt torque levels (see Table 6.4).

Figure 6.8 suggests that a non-zero intersection of radii-of-influence can be found such that the corresponding FE models predict their first four resonant frequencies within the lower and upper bounds determined experimentally. These predictions correspond to tied node radii of the FE models between 25.8 and 26.5 mm. The facts that, first, a range of radii-of-influence that meet our selection criteria is found and, second, the model reproduces the experimental trends, indicate that simplifying the parameterization to a single radius-of-influence suffices to establish positive test-analysis correlation. Therefore, more elaborate studies, where several radii are defined and varied independently, are not pursued.

6.6 Test-Analysis Correlation and Assessment of Bounding Predictions

The last part discusses the test-analysis correlation obtained from the measurement ranges assessed in Sect. 6.4 and prediction ranges of Sect. 6.5. The ranges of resonant frequencies obtained experimentally by varying the bolt torque, method of bolt tightening and sequence in which the bolts are tightened are compared to the ranges of numerical predictions obtained from parameter studies of the two "bounding-case" joint modeling strategies.

It is emphasized that our test-analysis correlation examines the "spread" of frequency values obtained with different model forms. This approach is different from a calibration study where, first, the model form is "frozen," and, second, parameters are optimized such that predictions reproduce the measurements as closely as possible. It would be possible to calibrate one FE model or another, however, our purpose is to quantify model-form uncertainty by evaluating the effect of implementing different representations of the structural joints.

Table 6.5 Ranges of measured and predicted resonant frequencies of the first four modes

	Measurements (Hz)		Contact stiffness model (Hz)		Tied node model (Hz)	
Resonant mode	Bounds	Range	Bounds	Range	Bounds	Range
1	58.8 − 71.6	12.8	53.8 − 73.1	19.3	43.5 − 70.4	26.9
2	97.5−103.0	5.5	65.8−101.2	35.4	65.5−100.5	35.0
3	102.0−106.0	4.0	100.4−106.2	5.8	93.2−105.3	12.1
4	170.0−193.0	23.0	168.5−198.3	29.8	148.0−191.7	43.7

Having said so, the calibration of model parameters is implicitly illustrated in Figs. 6.7 and 6.8. As indicated by the shaded regions of Fig. 6.7 (contact stiffness representation), different combinations of spring coefficients (k_{Bolt}; k_{Base}) provide "acceptable" predictions, that is, values located within the experimental ranges. Similarly in Fig. 6.8 for the tied node representation, different radii-of-influence lead to acceptable predictions. Of course, some of these predictions better reproduce the measurements than others. These results indicate the non-uniqueness of calibrated solutions.

Test-analysis correlation is summarized in Table 6.5 for the first four frequencies. The table lists the lower bounds, upper bounds and overall ranges of resonant frequencies. Bounds given in columns 2–3 for the measurements are identical to those of Table 6.4; they encompass the three bolt torque levels tested experimentally. For the FE predictions, the bounds reported are those obtained when parameters of the models are varied over their entire ranges.

Not captured in Table 6.5 is the fact that the contact stiffness representation is unable to predict all four frequencies with the same pair of parameters (k_{Bolt}; k_{Base}). Table 6.5 shows that the prediction ranges obtained from this model are able to fully "envelope" experimental measurements of the first, third and fourth modes. This is not the case for the second mode where the upper measurement bound is higher than the higher prediction bound. It suggests that the contact stiffness representation is incapable of capturing the torsional movement of the second mode, which is likely due to the fact that the rigidity/compliance conditions of the FE model are applied to the entire surfaces of the bracket-to-beam connections.

In contrast, the tied node representation is able to simultaneously capture all four frequencies for a range of radius-of-influence values. Table 6.5 shows that the model consistently provides lower bounds that are lower than those measured experimentally. This trend can be explained by the definition of the parametric study, which pursued radii ranging from 5 to 30 mm. The actual bolts of the portal frame are 12.7 mm in diameter, and the face of the brackets measures 63.5 mm by 50.8 mm. Table 6.5 also shows that the tied node representation is unable to predict resonant frequencies that are higher than the upper bounds of experimental measurements. As a result, predictions of this model do not "envelope" the measurements. This observation contrasts with results of the contact stiffness representation, which successfully encompasses measurements for three of the four vibration modes. We have verified that resonant frequencies predicted with large spring coefficients, that is, $k_{Bolt}, k_{Base} \geq 10^{+15}$ N/m, converge to values obtained when rigid connections are imposed over the entire contact surfaces of brackets. It suggests that restricting the tied node condition to a circular radius does not define a rigid-enough compliance that reproduces the experimental conditions. Allowing forces to be transmitted across the entire surface of the bracket-to-beam connection, as is done with a contact stiffness representation, is more appropriate to simulate high torque levels for the first, third and fourth vibration modes.

In summary, we are left with a modeling dilemma. The contact stiffness representation, that defines fictitious stiffness conditions between coincident nodes of the entire surface, is able to "envelope" the frequency measurements; it fails, however, to capture the torsion mode well. The tied node representation defines a physically more realistic description of the contact; it does not, however, provide enough rigidity especially when combined with high torque levels.

6.7 Conclusion

This report discusses the experimental and numerical analyses of the first four vibration modes of a nominally symmetric one-story portal frame structure. The experimental campaigns quantify variability due to changing the bolt torque, method by which the bolts are tightened, and sequence in which the bolts are tightened. The results support the idea that, as the torque is increased, the contact condition becomes more rigid, which causes the measured resonant frequencies to increase. Through analysis-of-variance, it is found that the bolt torque is the most influential factor for the second, third and fourth resonant frequencies. The first-mode frequency, that involves a shearing deformation, is equally influenced by the bolt torque and sequence in which the bolts are tightened. These findings drive the definition of modeling rules to represent the bracket-to-beam connections with two finite element models.

Table 6.6 Experimental, truncation, parameter and model-to-model uncertainties

		Contact stiffness model (Hz)		Tied node model (Hz)		
Resonant mode	Measurement range (Hz)	Truncation	Range	Truncation	Range	Model-to-model difference (Hz)
1	12.8	3.8	19.3	3.4	26.9	6.5
2	5.5	5.0	35.4	5.0	35.0	0.5
3	4.0	6.2	5.8	6.0	12.1	4.0
4	23.0	11.0	29.8	10.2	43.7	13.6

Two competing finite element models of the portal frame are developed using solid elements with differing assumptions to represent the joints: (1) contact stiffness coefficients and (2) tied nodes. Mesh refinement is executed to select an appropriate discretization. The contact stiffness representation defines fictitious springs between coincident nodes of the contact surfaces. All nodes of contact surfaces are connected in this manner. The tied node representation defines a tied constraint that does not permit relative displacement between coincident nodes located only within a radius-of-influence.

Parameter studies of the two competing models are pursued to assess the ranges of frequency predictions. The third resonant frequency of the out-of-phase bending mode is predicted by both models with the least variability. This is consistent with the experimental variability assessed from measurements. It is explained by the fact that this bending mode is more reliant on bolt properties than bolt torque level. When parameters of the contact stiffness representation are varied, predictions are able to "envelope" the experimental variability for the first, third and fourth resonant frequencies. This is not the case, however, for the second frequency of the torsion deformation mode. In comparison, the tied node representation gives frequency predictions that are consistent with the experimental variability for the four resonant modes considered. The tied node model is unable, however, to represent the upper range of experimental variability for any of the frequencies. In particular, neither joint modeling rule captures well the torsional mode at high bolt torque.

Table 6.6 gives a summary of various sources of uncertainty in the analysis of the portal frame. Column 2 lists the measurement ranges of resonant frequencies reported in Table 6.5. Columns 3–4 and 5–6 give the discretization and parametric ranges for the contact stiffness and tied node models, respectively. Differences between averaged frequency predictions of the two representations are listed in the last column. This simple metric quantifies model-form uncertainty, that is, the first-order effect on predictions of changing from the contact stiffness model to the tied node model.

The first observation from Table 6.6 is that, except for the second (torsional) mode, the model-form uncertainty (column 7) is comparable to truncation error (columns 3 and 5). It would be difficult to argue that one type of uncertainty is more significant than the other one. To achieve better prediction accuracy, one would need to simultaneously increase the level of resolution with which a calculation is performed, and implement a higher-fidelity representation of the joint. The close agreement between the two representations for the second frequency reflects the fact that neither model captures well the torsional deformation, especially at high bolt torque. The second observation from Table 6.6 is that, in all cases, varying model parameters produces larger prediction ranges than either truncation error or model-form uncertainty. We conclude that, for this particular application, model-form is not the main driver of prediction uncertainty. Calibration or small-scale experiments that focus on the joint dynamics would be needed to further reduce the unknown model parameter ranges.

Future work includes the development of models that better capture the torsional effects. One suggestion is to add point masses to the face of the top beam where bolt heads are located. Mass loading might affect the torsional deformation in ways that are different than varying the bolt torque level. Other model forms, such as discretizing the bolts with three-dimensional solid elements, can also be pursued.

This study demonstrates the benefits of implementing simplified modeling rules, however, only when the effects of these assumptions are studied and understood. This is what we propose through parameter studies and test-analysis correlation assessments of different model forms. We argue that this strategy yields a more thorough quantification of model-form uncertainty, instead of only relying on calibration to improve the accuracy of predictions.

Acknowledgements This work is performed under the auspices of the Los Alamos National Laboratory (LANL) as part of the Los Alamos Dynamics Summer School (LADSS). The authors are grateful to Dr. Charles Farrar, The Engineering Institute, for organizing the LADSS. The authors also wish to express their gratitude to Dr. Peter Avitabile, University of Massachusetts Lowell, for guidance in the experimental testing. The companies Simulia and Vibrant Technology, Inc., graciously contributed Abaqus and ME'Scope software licenses to the LADSS, without which this work would not have been possible. LANL is operated by the Los Alamos National Security, L.L.C., for the National Nuclear Security Administration of the U.S. Department of Energy under contract DE-AC52-06NA25396.

References

1. Alfaro JR, Arana I, Arazuri S, Jarén C (2010) Assessing the safety provided by SAE J2194 standard and code 4 standard code for testing ROPS, using finite element analysis. Biosyst Eng 105(2):189–197
2. ASCE (1998) Minimum design loads for buildings and other structures. American Society of Civil Engineers, Reston, VA
3. SAE J2940 (2011) Use of model verification and validation in product reliability and confidence assessments. Ground Vehicle Reliability Committee, Oct 2011
4. Det Norske Veritas (2010) Design and manufacture of wind turbine blades, offshore and onshore wind turbines, Oct 2010
5. Freebury G, Musial W (2000) Determining equivalent damage loading for full-scale wind turbine blade fatigue tests. In: 19th ASME wind energy symposium, Reno, Nevada
6. Freitas CJ (2002) The issue of numerical uncertainty. Appl Math Model 26(2):237–248
7. Mollineaux MG, Van Buren KL, Hemez FM, Atamturktur S (2013) Simulating the dynamics of wind turbine blades: Part I, Model development and verification. Wind Energy 16(5):694–710
8. Veldkamp D (2008) A probabilistic evaluation of wind turbine fatigue design rules. Wind Energy 11(6):655–672
9. Wilson GE, Boyack BE (1998) The role of the PIRT process in experiments, code development and code applications associated with reactor safety analysis. Nucl Eng Des 186(1–2):23–37
10. Chatfield C (1995) Model uncertainty, data mining, and statistical inference. J R Stat Soc A Stat Soc 158(3):419–466
11. Ewins DJ, Inman DJ (eds) (2000) Structural dynamics 2000: current status and future directions. Baldock Research Studies Press, Baldock
12. Segalman DJ, Gregory DL, Starr MJ, Resor BR, Jew MD, Lauffer JP, Ames NM (2009) Handbook on dynamics of jointed structures. Technical report SAND2009-4164, Sandia National Laboratories, Albuquerque, NM, July 2009
13. Hemez FM, Cornwell PJ, Avitabile P (2008) Validation of finite element predictions of the dynamic response of a frame structure. In: 26th SEM international modal analysis conference, Orlando, FL, 4–7 Feb 2008
14. Gonzales LM, Hall TM, Van Buren KL, Anton SR, Hemez FM (2013) Quantification of prediction bounds caused by model form uncertainty. Technical report LA-UR-13-27561, Los Alamos National Laboratory, Los Alamos, NM, Sept 2013